Improving the Performance of Spatial Modulation Full-Duplex Relaying System With Hardware Impairment Using Transmit Antenna Selection

BA CAO NGUYEN [ID][1], **TRAN MANH HOANG** [ID][1], **AND PHUONG T. TRAN** [ID][2], (Member, IEEE)

[1]Faculty of Radio Electronics, Telecommunications University, Nha Trang 650000, Vietnam
[2]Wireless Communications Research Group, Faculty of Electrical and Electronics Engineering, Ton Duc Thang University, Ho Chi Minh City 729000, Vietnam

Corresponding author: Phuong T. Tran (tranthanhphuong@ tdtu.edu.vn)

ABSTRACT This paper aims to study the impact of hardware impairments (HI) on the performance of spatial modulation (SM) system with full-duplex relay (FDR), namely SM-FDR system. To combat the negative effect of HI, a transmit antenna selection (TAS) scheme is applied at transmitter. The system performance in terms of outage probability (OP) and symbol error rate (SER) in case of HI and ideal hardware are compared. Furthermore, the impact of TAS on the system performance is also considered. This study derives successfully the exact expression of the OP and the approximate expression of the SER with TAS under the impact of both HI and residual self-interference (RSI). Both HI and RSI have strong influence on the performance of the SM-FDR system, especially at high data transmission rate, and the influence of the former is higher. However, the system performance is significantly enhanced, i.e. the SER is reduced, when TAS is applied. Therefore, it is recommended to apply TAS to improve the performance of SM-FDR systems when both HI and RSI exist in reality. Finally, all analytical expressions are validated by Monte Carlo simulation.

INDEX TERMS Hardware impairment (HI), full-duplex relay (FDR), self-interference cancellation (SIC), spatial modulation (SM), transmit antenna selection (TAS), outage probability (OP), symbol error rate (SER).

I. INTRODUCTION

Recently, the number of wireless devices has increased rapidly leading to higher requirements of wireless networks on high data transmission rate and connection reliability. In that context, many solutions have been proposed to improve the spectral efficiency such as full-duplex (FD), spatial modulation (SM), massive multiple-input multiple-output (MIMO), non-orthogonal multiple access (NOMA) [1]–[3]. In these techniques, FD communication has recently attracted increasing attention as it can double capacity compared to traditional half-duplex (HD) communication. In fact, FD devices can transmit and receive signals simultaneously and on the same frequency band while HD devices can only either transmit or receive signals at a specific time. However, FD performance is reduced due to residual self-interference (RSI) even after self-interference cancellation (SIC). Fortunately, the recent reports demonstrated that FD devices can remove up to 110 dB of self-interference (SI) power and then they can operate in realistic scenarios [4]–[6].

The associate editor coordinating the review of this manuscript and approving it for publication was Chunlong He [ID].

Additionally, relay communication has now found its application in various types of wireless networks such as the LTE-A mobile communication, ad hoc networks and vehicle-to-vehicle (V2V) networks. The combination of FD technique and relay network is now attractive and this system can be exploited for the future wireless networks, such as the fifth generation (5G) and beyond [7]–[9]. Therefore, various works have considered the impact of RSI on the performance of FDR systems in terms of outage probability (OP), symbol error rate (SER) and the ergodic capacity [7], [8], [10], [11]. These reports demonstrated that the performance of FDR systems is significantly degraded by RSI. Particularly, the OP and SER of the FDR systems go to some error floor at high SNR regime and cannot be reduced further [2], [3], [12]. To alleviate the effect of RSI, it is advisable to apply the optimal power allocation for FDR systems [8], [9], [11].

Beside FDR communications, MIMO systems increase capacity and reliability of wireless communication links compared to single-input single-output (SISO) systems [13], [14]. However, the multiple antennas in this system increase processing complexity of both transmitter and receiver. At the MIMO transmitter, power consumption is high because
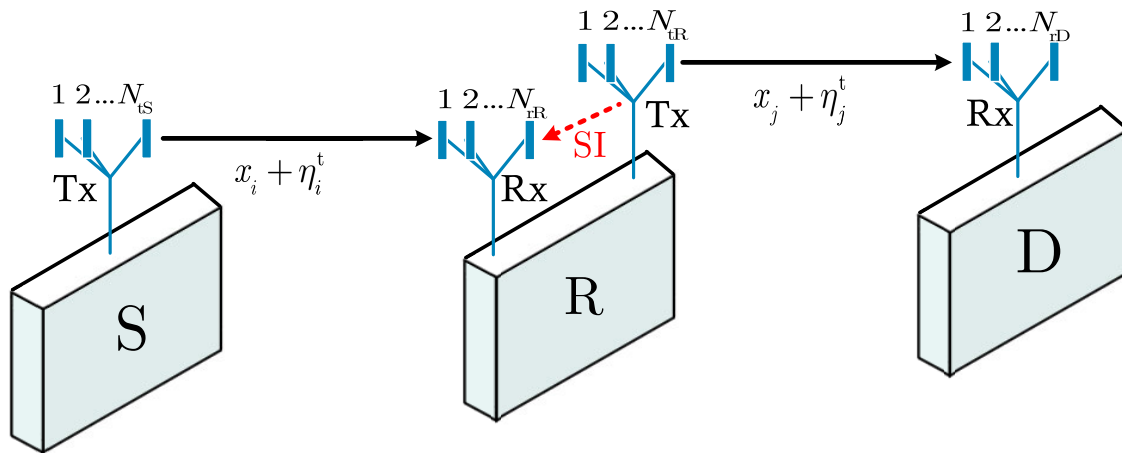
FIGURE 1. The system model of the considered TAS-SM-FDR system.

all transmit antennas are active to transmit the radio frequency (RF) signals. Moreover, the inter-channel interference (ICI) at the MIMO transmitter can reduce capacity and performance of MIMO systems. At the MIMO receiver side, the high complexity detectors are needed to process numerous received RF chains. To solve these above problems, spatial modulation (SM) has been proposed for MIMO systems. In SM-MIMO systems, the transmitted data bits are conveyed by both constellation point and the index of the activated transmit antenna. Consequently, only one symbol is transmitted, it means SM systems can avoid ICI and synchronization requirement at the transmitter. At the receiver, low-complexity Maximum-Likelihood (ML) detection can be implemented for signal decoding [13], [14]. As a result, the performance is improved while the complexity of computation and deployment are acceptable [15].

To increase the capacity of wireless communication systems, FDR and SM techniques have been combined in a system as in [7], [10], [15]–[17]. In these works, the performance of SM-FDR systems under the impact of RSI has been studied by analytical expressions such as OP, SER, and capacity. Moreover, both decode-and-forward (DF) and amplify-and-forward (AF) schemes are deployed for these studies. Their results shown a significant impact of RSI on the performance of SM-FDR systems. Particularly, the RSI level, which is a result from FD operation, was also considered in [15]. While the performance of SM-FDR systems has been widely studied in literature, the advantage of transmit antenna selection (TAS) has not been considered yet. In fact, the advantage of TAS has been demonstrated in [18]–[20] but only for half-duplex systems.

Furthermore, although a lot of works have studied the performance of SM-FDR system with ideal hardware, the transceiver hardware impairments (HI) have not been taken into account yet. In reality, they always exist in the system and reduce the performance of wireless systems, especially for low cost devices such as relay nodes [8], [21]–[24]. Motivated by these above facts, this paper proposes a TAS-SM-FDR scheme to overcome the effect of both HI and

RSI. The main contributions of this paper can be summarized as follows:

– The exact expression of signal-to-interference-plus-noise-and-distortion ratio (SINDR) of the TAS-SM-FDR system with HI at all nodes and RSI at FDR node over Rayleigh fading channel is derived successfully.

– The exact expression of OP and approximate expression of SER of the proposed system are also obtained from our analysis. These expressions can also be applied for ideal hardware case and half-duplex mode as two special cases.

– The benefits of applying TAS are analyzed. Based on numerical results, the system performance is significantly enhanced, i.e. SER is reduced when TAS is applied. In particular, SER of the TAS-SM-FDR system with HI is even better than that of ideal SM-FDR system without TAS. Furthermore, the impact of HI on the system performance is also rigourously investigated. It is found from the analysis that the effect of SI are more severe at high data rate regime and HI causes more trouble than RSI with the same level of power.

The rest of this paper is organized as follows. Section II presents the system model of the considered system with HI and RSI. Section III analyzes the system performance with TAS in terms of OP and SER. Numerical results and discussion are provided in Section IV and finally, Section V concludes the paper.

II. SYSTEM MODEL

Fig. 1 illustrates a three-node network topology of our proposed TAS-SM-FDR system. All three nodes in this system, including the source node S, the relay node R, and the destination node D, are equipped with multiple antennas. Both S and D operate in HD communication mode, where N_{tS} and N_{rD} denote the number of transmit antennas of S and the number of receive antennas of D, respectively. It is assumed that there is no direct link from S to D due to far distance and deep shadow fading. Therefore, data is transmitted from S to D with the help of the relay R. R operates in FD mode and follows the decode-and-forward (DF) strategy, with N_{tR} transmit antennas and N_{rR} receive antennas. With FD

capability, R can transmit and receive signals simultaneously and on the same frequency band. Consequently, there exists some self-interference at the receiving antennas caused by the transmit signal of R itself. With the knowledge about its own signal, the relay R may apply various SIC techniques such as antenna domain suppression or analog and digital domain cancellation to suppress this interference to a certain level. It is noted that in reality, R can use shared-antennas for both transmission and reception by using a circulator [4]. However, using separate antennas for transmission and reception can efficiently alleviate the impact of SI, especially by applying the antenna domain suppression method. In fact, it is easy to deploy various methods in antenna domain for separating the antennas such as isolation, placing absorptive shielding, cross-polarization and directional transmission antennas [25].

A. IDEAL HARDWARE CASE

Our analysis starts with the ideal hardware case for SM-FDR system. The received signals at R and D in this case are respectively expressed as

$$\mathbf{y}_R = \mathbf{h}_{iR} x_i + \tilde{\mathbf{h}}_{jR} x_j + \mathbf{z}_R, \qquad (1)$$

$$\mathbf{y}_D = \mathbf{h}_{jD} x_j + \mathbf{z}_D, \qquad (2)$$

where $\mathbf{h}_{iR} \in \mathbb{C}^{N_{rR} \times 1}$ and $\mathbf{h}_{jD} \in \mathbb{C}^{N_{rD} \times 1}$ are respectively the channel vectors from ith transmit antenna of S to N_{rR} receive antennas of R and from jth transmit antenna of R to N_{rD} receive antennas of D; $\tilde{\mathbf{h}}_{jR} \in \mathbb{C}^{N_{rR} \times 1}$ is self-interference channel vector from jth transmit antenna to N_{rR} receive antennas of R; $x_i(t) \in \mathbb{C}^{N_{rR} \times 1}$ and $x_j(t) \in \mathbb{C}^{N_{rD} \times 1}$ are transmitted signals from ith antenna of S and jth antenna of R, respectively; $\mathbf{z}_R(t) \in \mathbb{C}^{N_{rR} \times 1}$ and $\mathbf{z}_D(t) \in \mathbb{C}^{N_{rD} \times 1}$ are Gaussian noise vectors at R and D, respectively, with zero mean and variance of σ_R^2, σ_D^2, respectively, i.e. $\mathbf{z}_R \sim \mathcal{CN}(0, \sigma_R^2)$ and $\mathbf{z}_D \sim \mathcal{CN}(0, \sigma_D^2)$.

Because SM is employed in our model, only one antenna is active among N_{tS} transmit antennas of S and only one antenna is active among N_{tR} transmit antennas of R. Therefore, the channel vectors $\mathbf{h}_{iR}$ and $\mathbf{h}_{jD}$ are expressed as

$$\mathbf{h}_{iR} = \begin{bmatrix} h_{i1} & h_{i2} & \dots & h_{iN_{rR}} \end{bmatrix}^T, \qquad (3)$$

$$\mathbf{h}_{jD} = \begin{bmatrix} h_{j1} & h_{j2} & \dots & h_{jN_{rD}} \end{bmatrix}^T, \qquad (4)$$

where $i \in \{1, 2, \dots, N_{tS}\}$ and $j \in \{1, 2, \dots, N_{tR}\}$.

B. HARDWARE IMPAIRMENT CASE

In case of imperfect hardware, the impairments in physical transceiver create distortion noise at both transmitter and receiver. Hence, the received signals at R and D in this case are respectively given as

$$\mathbf{y}_R = \mathbf{h}_{iR}(x_i + \eta_S^t) + \tilde{\mathbf{h}}_{jR}(x_j + \eta_R^t) + \boldsymbol{\eta}_R^r + \mathbf{z}_R, \qquad (5)$$

$$\mathbf{y}_D = \mathbf{h}_{jD}(x_j + \eta_R^t) + \boldsymbol{\eta}_D^r + \mathbf{z}_D, \qquad (6)$$

where η_S^t and η_R^t are the distortion noises caused by transmitter impairments at S and R, respectively; $\boldsymbol{\eta}_R^r$ and $\boldsymbol{\eta}_D^r$ are the distortion noise vectors due to receiver impairments at R

and D, respectively. These hardware noise terms are modeled as complex Gaussian distributed random variables or vectors [21], [23], [24]. In particular, we have $\eta_S^t \sim \mathcal{CN}(0, (k_S^t)^2 P_S)$ and $\eta_R^t \sim \mathcal{CN}(0, (k_R^t)^2 P_R)$, where k_S^t and k_R^t denote the levels of hardware impairment at the transmitters S and R, respectively. Similarly, $\boldsymbol{\eta}_R^r \sim \mathcal{CN}(0, \|\mathbf{h}_{iR}\|^2(k_R^r)^2 P_S)$ and $\boldsymbol{\eta}_D^r \sim \mathcal{CN}(0, \|\mathbf{h}_{jD}\|^2(k_D^r)^2 P_R)$, where k_R^r and k_D^r denote the levels of the hardware impairment at the receivers R and D, respectively.

The term $\tilde{\mathbf{h}}_{jR}(x_j + \eta_R^t)$ in (5) represents the self-interference originated from FD communication. Due to imperfect hardware and SI channel estimation error, SIC techniques at R may not remove SI completely. Let $\mathbf{r}_{SI}$ denote the RSI at the FD relay R after applying various SIC techniques, which can be modeled as a complex Gaussian variable [2], [7], [12], [23], [26] with zero-mean and variance of σ_{RSI}^2, where $\sigma_{RSI}^2 = l^2 P_R$. Here, l represents the SIC capability at R.

Now, the received signal at R can be rewritten as

$$\mathbf{y}_R = \mathbf{h}_{iR}(x_i + \eta_S^t) + \boldsymbol{\eta}_R^r + \mathbf{r}_{SI} + \mathbf{z}_R, \qquad (7)$$

When TAS is applied for SM system, a set of transmit antennas is selected from all available antennas at the transmitters. Specifically, we assume that J_S and J_R are the sets of transmit antennas selected at S and R, respectively. Herein, J_S and J_R must satisfy $|J_S| \leq N_{tS}$, $|J_S| = 2^p$, $|J_R| \leq N_{tR}$, and $|J_R| = 2^q$, where p and q are positive integers. The reason for the power of two is as follows. For SM, the input bit sequence is mapped to the antenna indices. Further, spatial modulator selects the transmit antenna using the mapped antenna index. Thus, the number of antennas in the selected set is equal to the number of symbols in the data alphabet, which is a power of two. In other words, the transmit antenna is varying according to the input binary stream [27]. The ultimate goal for selecting J_S and J_R is to maximize the total received signal power. For example, let's consider $\mathbf{h}_{jD}$ with $q = 2$ (binary symbol). Assume that the norms of the channel coefficients satisfy

$$\|\mathbf{h}_{1D}\|^2 \geq \|\mathbf{h}_{2D}\|^2 \geq \|\mathbf{h}_{3D}\|^2 \geq \dots \geq \|\mathbf{h}_{N_{tR}D}\|^2, \qquad (8)$$

where $\mathbf{h}_{1D}, \mathbf{h}_{2D}, \dots, \mathbf{h}_{N_{tR}D}$ are calculated from (4). For binary symbol transmission, two antennas are selected, i.e., $|J_R| = 2$. From (8), we can select J_R as

$$J_R = \{\|\mathbf{h}_{1D}\|^2, \|\mathbf{h}_{2D}\|^2\}. \qquad (9)$$

Based on that, either first or second antenna is active for transmitting signals from R to D depending on the incoming data bits, i.e., the first antenna is active to transmit "0" bit and the second antenna is active to transmit "1" bit.

From (7), the instantaneous SINDR at R (denoted by γ_R) is computed as

$$\gamma_R = \frac{\|\mathbf{h}_{iR}\|^2 P_S}{\|\mathbf{h}_{iR}\|^2 (k_S^t)^2 P_S + \|\mathbf{h}_{iR}\|^2 (k_R^r)^2 P_S + \sigma_{RSI}^2 + \sigma_R^2}$$

$$= \frac{\|\mathbf{h}_{iR}\|^2 P_S}{\|\mathbf{h}_{iR}\|^2 k_S^2 P_S + \sigma_{RSI}^2 + \sigma_R^2} = \frac{\|\mathbf{h}_{iR}\|^2 \bar{\gamma}_R}{\|\mathbf{h}_{iR}\|^2 k_S^2 \bar{\gamma}_R + 1}, \qquad (10)$$

where $k_S^2 = (k_S^t)^2 + (k_R^r)^2$ is the aggregated HI level, which combines both HI terms at the transmitter S (k_S^t) and the receiver R (k_R^r), and $\bar{\gamma}_R \triangleq \frac{P_S}{\sigma_{RSI}^2 + \sigma_R^2}$.

Similarly, based on (6), the instantaneous SINDR at D (denoted by γ_D) is computed as

$$
\begin{aligned}
\gamma_D &= \frac{\|\mathbf{h}_{jD}\|^2 P_R}{\|\mathbf{h}_{jD}\|^2 (k_R^t)^2 P_R + \|\mathbf{h}_{jD}\|^2 (k_D^r)^2 P_R + \sigma_D^2} \\
&= \frac{\|\mathbf{h}_{jD}\|^2 P_R}{\|\mathbf{h}_{jD}\|^2 k_R^2 P_R + \sigma_D^2} = \frac{\|\mathbf{h}_{jD}\|^2 \bar{\gamma}_D}{\|\mathbf{h}_{jD}\|^2 k_R^2 \bar{\gamma}_D + 1}, \quad (11)
\end{aligned}
$$

where $k_R^2 = (k_R^t)^2 + (k_D^r)^2$ is the aggregated HI level which combines of both HI at the transmitter R (k_R^t) and the receiver D (k_D^r), and $\bar{\gamma}_D \triangleq \frac{P_R}{\sigma_D^2}$.

With DF protocol at FD relay, the end-to-end SINDR (denoted by γ_{e2e}) of the considered system can be determined as

$$
\gamma_{e2e} = \min\{\gamma_R, \gamma_D\}, \quad (12)
$$

where γ_R and γ_D are given in (10) and (11), respectively.

III. PERFORMANCE ANALYSIS

A. OUTAGE PROBABILITY ANALYSIS

The outage probability is defined as the probability that makes the instantaneous data transmission rate of the considered system falling below a predefined data rate [28]. For SM system, the information bits are embedded in both the transmitted symbol and the index of the transmit antenna. Therefore, in general the capacity of SM systems is higher than that of single-input multiple-output (SIMO) systems [7], [13].

For the considered TAS-SM-FDR system, the OP is computed by

$$
\mathcal{P}_{out} = \Pr\{\mathcal{R}_{SM} < \mathcal{R}_0\}, \quad (13)
$$

where $\mathcal{R}_{SM}$ and $\mathcal{R}_0$ are the instantaneous data transmission rate and predefined data transmission rate of the considered system, respectively. Herein, $\mathcal{R}_{SM}$ is calculated as

$$
\mathcal{R}_{SM} = \log_2(N_t) + \log_2(1 + \gamma), \quad (14)
$$

where N_t presents the number of transmit antennas at the transmitter ($N_t = N_{tS}$ for S and $N_t = N_{tR}$ for R) and γ is SINDR at the receivers, i.e., γ_R or γ_D. It is also noted that, because DF policy is used at the FD relay, a system outage event occurs when either S – R link or R – D link cannot afford the predefined data transmission rate.

As a result, an outage event occurs when

$$
\begin{aligned}
&\log_2(N_{tS}) + \log_2(1 + \gamma_R) < \mathcal{R}_0 \\
\text{or} \quad &\log_2(N_{tR}) + \log_2(1 + \gamma_D) < \mathcal{R}_0. \quad (15)
\end{aligned}
$$

As can be seen from (15), when the S – R link is in outage, the system outage event occurs, regardless of the fact that the R – D link is in outage or not. When the S – R link is not in outage, that means the SNR of the first hop is above a certain threshold, the system outage event occurs when the R – D link is in outage.

(15) can be written equivalently as

$$
\gamma_R < 2^{\mathcal{R}_0 - \log_2(N_{tS})} - 1 \text{ or } \gamma_D < 2^{\mathcal{R}_0 - \log_2(N_{tR})} - 1. \quad (16)
$$

Let $\mathcal{R}_1 = \mathcal{R}_0 - \log_2(N_{tS})$ and $\mathcal{R}_2 = \mathcal{R}_0 - \log_2(N_{tR})$ be respectively the instantaneous data transmission rates due to modulation orders of S − R and R − D links. The OP is then defined as

$$
\mathcal{P}_{out} = \Pr\{(\gamma_R < 2^{\mathcal{R}_1} - 1) \cup (\gamma_D < 2^{\mathcal{R}_2} - 1)\}. \quad (17)
$$

By denoting two thresholds as $\gamma_{th1} \triangleq 2^{\mathcal{R}_1} - 1$ and $\gamma_{th2} \triangleq 2^{\mathcal{R}_2} - 1$, (17) becomes

$$
\begin{aligned}
\mathcal{P}_{out} &= \Pr\{(\gamma_R < \gamma_{th1}) \cup (\gamma_D < \gamma_{th2})\} \\
&= \Pr\{(\gamma_R < \gamma_{th1})\} + \Pr\{(\gamma_D < \gamma_{th2})\} \\
&\quad - \Pr\{(\gamma_R < \gamma_{th1})\}\Pr\{(\gamma_D < \gamma_{th2})\}, \quad (18)
\end{aligned}
$$

because $\{\gamma_R < \gamma_{th1}\}$ and $\{\gamma_D < \gamma_{th2}\}$ are two independent events.

From (18), the OP of the considered TAS-SM-FDR system is obtained in the following theorem.

Theorem 1: Under the impact of both HI and RSI, the outage probability expression of the considered TAS-SM-FDR system over Rayleigh fading channel is given by

$$
\mathcal{P}_{out} = \begin{cases} \mathcal{P}_{out_1} + \mathcal{P}_{out_2} - \mathcal{P}_{out_1}\mathcal{P}_{out_2}, & \text{if } \begin{cases} \gamma_{th1} < 1/k_S^2 \\ \gamma_{th2} < 1/k_R^2 \end{cases} \\ 1, & \text{otherwise} \end{cases} \quad (19)
$$

where $\mathcal{P}_{out_1}$ and $\mathcal{P}_{out_2}$ are derived in (20) and (21), as shown at the bottom of the next page, $\chi_R = \frac{\gamma_{th1}}{2\bar{\gamma}_R(1 - k_S^2\gamma_{th1})}(1 + \phi_m)$, $\chi_D = \frac{\gamma_{th2}}{2\bar{\gamma}_D(1 - k_R^2\gamma_{th2})}(1 + \phi_n)$, $w_S = N_{tS} - |J_S| + 1$, $w_R = N_{tR} - |J_R| + 1$; $B(.,.), \Gamma(.)$ and $\Gamma(.,.)$ are the beta, gamma, and incomplete gamma functions [29], respectively; M and N are the complexity-accuracy trade-off parameters [30] for calculating $\mathcal{P}_{out_1}$ and $\mathcal{P}_{out_2}$, respectively; $\phi_m = \cos\left(\frac{(2m-1)\pi}{2M}\right)$ and $\phi_n = \cos\left(\frac{(2n-1)\pi}{2N}\right)$.

It should be better to know that we use the incomplete gamma function instead of a finite series to reduce the length of the derived mathematical expressions. In fact, from the obtained expressions, we can rewrite these expressions without the incomplete gamma function via replacing the incomplete gamma function by a finite series such as in Appendix A because the parameters are integers.

Proof 1: The detailed proof of this theorem is presented in Appendix A.

B. SYMBOL ERROR RATE ANALYSIS

For wireless system, many approximations or exact values of the SER derived for coherent modulation are given in the following form [28]:

$$
\text{SER} = a\mathbb{E}\{Q(\sqrt{b\gamma})\} = \frac{a}{\sqrt{2\pi}} \int_0^\infty F\left(\frac{t^2}{b}\right) e^{-\frac{t^2}{2}} dt, \quad (22)
$$

where a and b are constants that depend on the modulation types, for example, $(a, b) = (1, 2)$ and $(a, b) = (2, 1)$ for

binary phase-shift keying (BPSK) and 4-quadrature amplitude modulation (4-QAM) modulations, respectively [28]. Notice that the values of a and b for different modulation schemes are determined using Table 6.1 of [28]; $Q(x) \triangleq \frac{1}{\sqrt{2\pi}} \int_x^\infty e^{-t^2/2} dt$ is the Gaussian function; γ and $F(x)$ are respectively the end-to-end SINDR of the system and its CDF.

By letting $x = \frac{t^2}{b}$, we can rewrite (22) as

$$\text{SER} = \frac{a\sqrt{b}}{2\sqrt{2\pi}} \int_0^\infty \frac{e^{-bx/2}}{\sqrt{x}} F(x) dx. \tag{23}$$

From (23), the SER of the considered TAS-SM-FDR system can be found in Theorem 2 as follows.

Theorem 2: The SER *of the considered TAS-SM-FDR system (using the coherent modulation schemes mentioned above) under the impact of both HI and RSI is computed as*

$$\text{SER} \approx \frac{a\sqrt{b}}{2\sqrt{2\pi}} \left[\text{SER}_{S,R} + \text{SER}_{R,D} - \text{SER}_3 \right.$$
$$\left. + \sqrt{\frac{2\pi}{b}} \left(1 - \text{erf}\left(\sqrt{\frac{b\Delta}{2}} \right) \right) \right], \tag{24}$$

where $\text{SER}_{S,R}$, $\text{SER}_{R,D}$ *are given as in* (25)*, as shown at the bottom of the next page, and* SER_3 *is given by* (26)*, as shown at the bottom of the next page;* C *is the complexity-accuracy trade-off parameter for calculating SER;* $\phi_c = \cos\left(\frac{(2c-1)\pi}{2C} \right)$, $\psi_R = \frac{1}{2\bar{\gamma}_R}(1 + \phi_m)$, $\psi_D = \frac{1}{2\bar{\gamma}_D}(1 + \phi_n)$, $u = \frac{\Delta}{2}(1 + \phi_c)$, *and* $\Delta = \min\left(\frac{1}{k_S^2}, \frac{1}{k_R^2} \right)$.
for $(A, B) \in \{(S, R), (R, D\}$ *and* $C_{S,R} = M, C_{R,D} = N, \phi_{S,R} = \phi_m, \phi_{R,D} = \phi_n$.

Proof 2: The detailed proof of Theorem 2 can be found in Appendix B.

IV. NUMERICAL RESULTS AND DISCUSSIONS
In this section, the performance of the TAS-SM-FDR system with HI is evaluated by using analytical expressions in Theorem 1 and Theorem 2, and also verified by Monte Carlo simulations. To clearly indicate the impact of HI on the OP and SER of the considered system, we simulate the OP and SER of the SM-FDR system with ideal hardware first. Then,

TABLE 1. Simulation parameters.

Symbol	Parameter name	Fixed value	Varying range
N_t	Number of transmitting antennas	4	4, 6, 8
N_r	Number of receiving antennas	2	none
J	Size of TAS sets	2	none
SNR	Transmit-power-to-noise-ratio	30 dB	$0 \to 20$ dB
k	HI level	0.15	$0.05 \to 0.3$
l	RSI level	0.15	$0.05 \to 0.3$
$\mathcal{R}$	Desired data rate	3; 4 bps/Hz	none

the OP and SER of SM-FDR system with imperfect hardware but without TAS are also investigated to demonstrate the benefits of TAS. The impact of different parameters, including transmit-power-to-noise-ratio SNR, desired data rate $\mathcal{R}$, HI and RSI level k and l, and number of transmit and receive antennas, on the outage performance is illustrated in this section. We respectively let one of these parameters vary in a certain range while fixing all other parameters. For simplicity, we set the same average transmit power at the transmitters $P_S = P_R = P$, the same variance of noises at all nodes $\sigma_R^2 = \sigma_D^2 = \sigma^2$, the same number of transmit (receive) antennas at all transmitting (receiving) nodes $N_{tS} = N_{tR} = N_t$ and $N_{rR} = N_{rD} = N_r$, the same size of TAS sets $|J_S| = |J_R| = J = 2$, the same HI levels at all nodes $k_S^t = k_R^t = k_R^r = k_D^r = k$, the complexity-accuracy trade-off parameters are $M = N = C = 10$, and define SNR $\triangleq P/\sigma^2$. The chosen values of simulation parameters are listed in Table 1. It is noted that in Fig. 2, notations "Wi" and "Wo" denote the case with and without TAS, respectively.

Fig. 2 investigates the OPs of the SM-FDR system under imperfect hardware with and without TAS. Equation (19) in Theorem 1 is used to plot the OP of the TAS-SM-FDR system with HI. The OPs of ideal SM-FDR with and without TAS are also plotted on Fig. 2 by analysis and simulation to show the performance difference between the HI and ideal hardware cases. It is clear to see that, the impact of HI is more severe for higher data transmission rate. The difference between the OPs of ideal and non-ideal SM-FDR systems in the case of $\mathcal{R} = 4$ is larger than that in the case of $\mathcal{R} = 3$, either with or without TAS. Fig. 2 shows a strong impact of HI on the OP of SM-FDR system. In the case of $\mathcal{R} = 3$ bit/s/Hz and

$$\mathcal{P}_{out_1} = \frac{\pi \gamma_{th1}}{2M(N_{tS} - w_S + 1)\Gamma(N_{rR})\bar{\gamma}_R(1 - k_S^2\gamma_{th1})} \sum_{p=w_S}^{N_{tS}} \sum_{m=1}^{M} \frac{\sqrt{1 - \phi_m^2}}{B(p, N_{tS} - p + 1)}$$
$$\times \left(1 - \frac{\Gamma(N_{rR}, \chi_R)}{\Gamma(N_{rR})} \right)^{p-1} \left(\frac{\Gamma(N_{rR}, \chi_R)}{\Gamma(N_{rR})} \right)^{N_{tS}-p} \chi_R^{N_{rR}-1} e^{-\chi_R}. \tag{20}$$
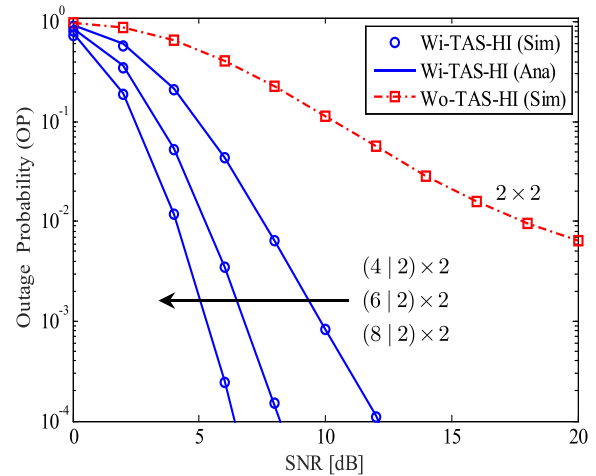
$$\mathcal{P}_{out_2} = \frac{\pi \gamma_{th2}}{2N(N_{tR} - w_R + 1)\Gamma(N_{rD})\bar{\gamma}_D(1 - k_R^2\gamma_{th2})} \sum_{q=w_R}^{N_{tR}} \sum_{n=1}^{N} \frac{\sqrt{1 - \phi_n^2}}{B(q, N_{tR} - q + 1)}$$
$$\times \left(1 - \frac{\Gamma(N_{rD}, \chi_D)}{\Gamma(N_{rD})} \right)^{q-1} \left(\frac{\Gamma(N_{rD}, \chi_D)}{\Gamma(N_{rD})} \right)^{N_{tR}-q} \chi_D^{N_{rD}-1} e^{-\chi_D}. \tag{21}$$
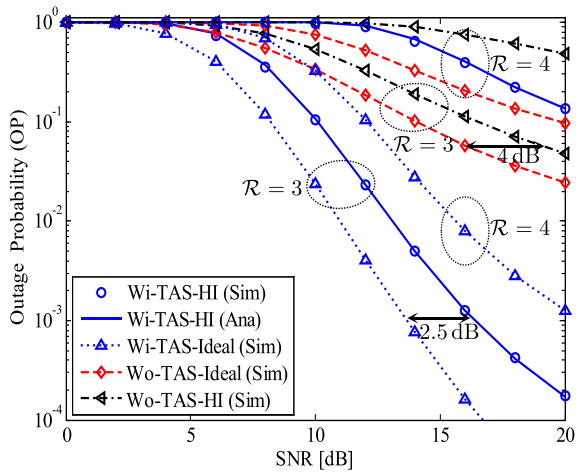
FIGURE 2. The OPs of SM-FDR systems with ideal and non-ideal hardware, with and without TAS versus the average SNR with $N_t = 4$, $N_r = 2$, $J = 2$, $\mathcal{R} = 3$, 4 bit/s/Hz; the HI and RSI levels are $k = l = 0.15$.

FIGURE 3. The OP of the SM-FDR system under HI with and without TAS with difference of number of transmission antennas at S and R.

$OP = 10^{-3}$, the ideal SM-FDR system has the gains of 2.5 dB and 4 dB in the SNR (to achieve the same OP performance) compared to the imperfect harware SM-FDR system with and without TAS, respectively. When the data transmission rate increases, i.e., $\mathcal{R} = 4$ bit/s/Hz, the SNR gains in the case of ideal hardware compared to the case of HI are increased (either with or without TAS). Therefore, when HI exists in the system, it is necessary to use suitable data transmission rate for the SM-FDR system to avoid decreasing the performance. On the other hand, it is shown that TAS significantly improves the performance of SM-FDR systems in case of HI. With $\mathcal{R} = 3$ bit/s/Hz and SNR = 20 dB, the TAS-SM-FDR system with HI has OP = 2×10^{-4} with TAS while OP = 8×10^{-2} for the non-TAS case.

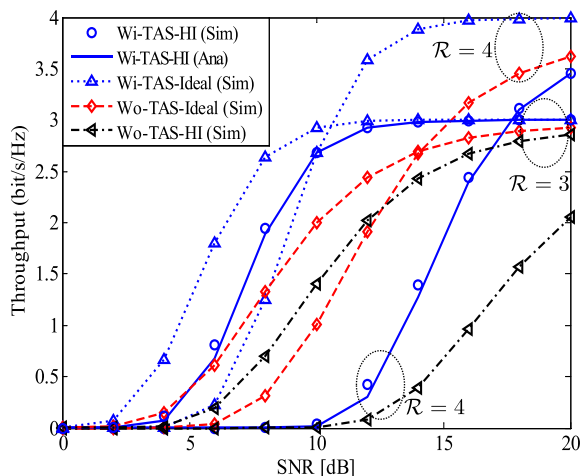Fig. 3 illustrates the OPs of the TAS-SM-FDR system with various antenna configurations at S and R, i.e., with

the number of transmit antennas $N_t = 4, 6, 8$, respectively. Here, we set $\mathcal{R} = 2$ bit/s/Hz. In Fig. 3, we use the notation form $(N_t|J) \times N_r$ to describe the antenna configuration, where N_t is the number of transmit antennas, J is the number of selected antennas, and N_r is the number of receive antennas. For example, $(6|2) \times 2$ means $N_t = 6$, $J = 2$, and $N_r = 2$. If TAS is not employed, the above SM-FDR system becomes a system with two transmit and receive antennas and is denoted by 2×2 ($N_t = 2$ and $N_r = 2$). Fig. 3 demonstrates the benefit of using TAS-SM-FDR system in the case of imperfect hardware. It can be observed that the system OP without TAS nearly reaches 10^{-2} at SNR = 20 dB while with TAS, OP = 10^{-4} at SNR = 6, 8, 12 dB for $(8|2) \times 2$, $(6|2) \times 2$ and $(4|2) \times 2$ configurations, respectively. In addition, without TAS, the OP slowly reduces at high SNR region and reaches an outage floor due to the impact

$$SER_{A,B} = \frac{\pi^2 \Delta}{4 C_{A,B} C (N_{tA} - w_A + 1) \Gamma(N_{rB}) \bar{\gamma}_B} \sum_{p=w_A}^{N_{tA}} \sum_{m=1}^{C_{A,B}} \sum_{c=1}^{C} \frac{\psi_B^{N_{rB}-1} \sqrt{(1 - \phi_{A,B}^2)(1 - \phi_c^2)}}{B(p, N_{tA} - p + 1)}$$

$$\times \left(1 - \frac{\Gamma(N_{rB}, \frac{\psi_B u}{1 - k_A^2 u})}{\Gamma(N_{rB})} \right)^{p-1} \left(\frac{\Gamma(N_{rB}, \frac{\psi_B u}{1 - k_A^2 u})}{\Gamma(N_{rB})} \right)^{N_{tA}-p} e^{-\frac{\psi_B u}{1 - k_A^2 u} - \frac{bu}{2}} \frac{u^{N_{rB} - \frac{1}{2}}}{(1 - k_A^2 u)^{N_{rB}}} \quad (25)$$

$$SER_3 = \frac{\pi^3 \Delta}{8 MNC (N_{tS} - w_S + 1)(N_{tR} - w_R + 1) \Gamma(N_{rR}) \Gamma(N_{rD}) \bar{\gamma}_R \bar{\gamma}_D} \sum_{p=w_S}^{N_{tS}} \sum_{m=1}^{M} \sum_{q=w_R}^{N_{tR}} \sum_{n=1}^{N} \sum_{c=1}^{C} \frac{\psi_R^{N_{rR}-1} \psi_D^{N_{rD}-1}}{B(p, N_{tS} - p + 1)}$$

$$\times \frac{e^{-\frac{\psi_R u}{1 - k_S^2 u} - \frac{\psi_D u}{1 - k_R^2 u} - \frac{bu}{2}} \sqrt{(1 - \phi_m^2)(1 - \phi_n^2)(1 - \phi_c^2)}}{B(q, N_{tR} - q + 1)(1 - k_S^2 u)^{N_{rR}}(1 - k_R^2 u)^{N_{rD}}} \left(1 - \frac{\Gamma(N_{rR}, \frac{\psi_R u}{1 - k_S^2 u})}{\Gamma(N_{rR})} \right)^{p-1} \left(\frac{\Gamma(N_{rR}, \frac{\psi_R u}{1 - k_S^2 u})}{\Gamma(N_{rR})} \right)^{N_{tS}-p}$$

$$\times \left(1 - \frac{\Gamma(N_{rD}, \frac{\psi_D u}{1 - k_R^2 u})}{\Gamma(N_{rD})} \right)^{q-1} \left(\frac{\Gamma(N_{rD}, \frac{\psi_D u}{1 - k_R^2 u})}{\Gamma(N_{rD})} \right)^{N_{tR}-q} \quad (26)$$

FIGURE 4. The impact of HI on the throughput of the SM-FDR system under HI with and without TAS in comparison with the throughput of ideal SM-FDR system.

FIGURE 5. The SER of the considered SM-FDR system with HI versus the average SNR using 4-QAM modulation.

FIGURE 6. The SER of the SM-FDR system with HI versus the RSI level for the case with and without TAS, $k = 0.15$.

of both HI and RSI. Meanwhile, the OP when TAS is applied is rapidly reduced, so the performance of the TAS-SM-FDR system is greatly enhanced.

Fig. 4 investigates the impact of HI on the throughput of the considered system in comparison with the ideal hardware case, where the throughput $\mathcal{T}$ of the system is defined as $\mathcal{T} = \mathcal{R}(1 - \mathcal{P}_{\text{out}})$, with $\mathcal{P}_{\text{out}}$ is given by (19) for TAS-SM-FDR system. In the case of $\mathcal{R} = 3$ bit/s/Hz, TAS-SM-FDR system can reach the target throughput 3 bit/s/Hz at SNR = 14 dB for both ideal and non-ideal hardware cases. However, for the non-TAS case, the throughput of SM-FDR system in both ideal and non-ideal cases reaches the target value of 3 bit/s/Hz at SNR = 20 dB. For higher data transmission rate, i.e., $\mathcal{R} = 4$ bit/s/Hz, only the case of TAS-SM-FDR system with ideal hardware can achieve the target throughput 4 bit/s/Hz at SNR = 16 dB. For all remaining cases, the target throughput 4 bit/s/Hz cannot be achieved for the considered SNR range. From Fig. 2 and Fig. 4, it is obvious that TAS significantly improves both OP performance and throughput of SM-FDR systems with HI.

Fig. 5 illustrates the SER of the considered TAS-SM-FDR system using 4-QAM modulation ($a = 2, b = 1$). Other parameters for obtaining Fig. 5 are similar to the ones in Fig. 2. Here, (24) in Theorem 2 is used to plot the analytical curve of the TAS-SM-FDR system with HI and Monte Carlo simulation is conducted to obtain the corresponding simulation curve. Similar to OP, SER can be reduced significantly by applying TAS. As seen from Fig. 5, the analysis curve and simulation curve perfectly match, except for low SNR regime, where there is a slight difference between analysis and simulation. When SNR = 30 dB, the SER of the TAS-SM-FDR system with HI and the SERs of the ideal or non-ideal hardware SM-FDR systems without TAS go to the error floor due to the impact of both HI and RSI. Only the SER of the TAS-SM-FDR system with ideal hardware can avoid the error
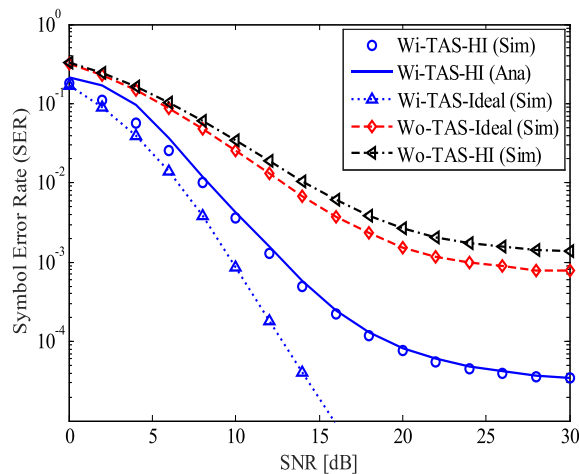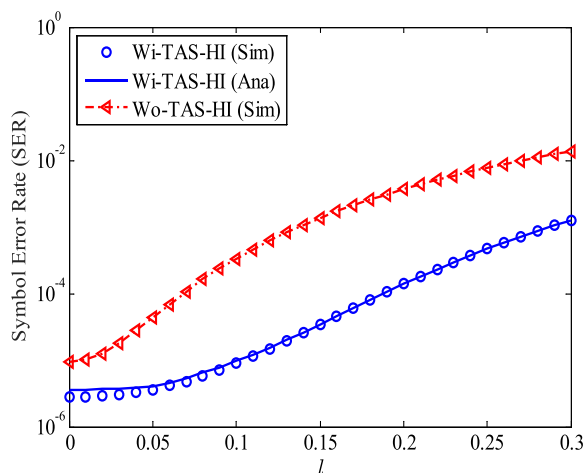
floor for the simulation range. At the error floor, SER of the TAS-SM-FDR system with HI is nearly 100 times lower than that of non-TAS SM-FDR system. This confirms again the benefit of using TAS for the SM-FDR system with HI.

Fig. 6 considers SER of SM-FDR systems with HI versus the RSI level l for the cases with and without TAS. Here, the HI level is set to $k = 0.15$ and SNR is fixed at 30 dB. The RSI power is calculated as $\sigma_{\text{RSI}}^2 = l^2 P_R$, so σ_{RSI}^2 is an increasing function with respect to l. In the case of $l = 0$, the SER of the SM-FDR system with HI becomes the SER of the SM-HDR system with HI. It can be observed that the impact of l on SERs of the TAS-SM-FDR and non-TAS SM-FDR systems with imperfect hardware are similar because two curves are almost parallel. Compare with the SER of the SM-HDR system ($l = 0$), the SER of the SM-FDR system is 10 and 100 times higher for the cases of $l = 0.15$ and $l = 0.3$, respectively. Therefore, a considerable effort is required to achieve better RSI suppression.
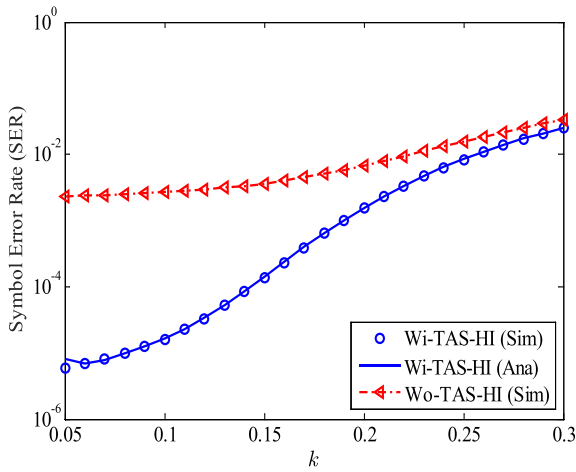
FIGURE 7. The impact of HI level on the SER performance of the SM-FDR system under HI with and without TAS, *l* = 0.15.

Fig. 7 investigates the impact of HI level k on the SER of the considered system with and without TAS when the RSI level is $l = 0.15$ and SNR = 30 dB. When the HI level is small, i.e., $k = 0.05$, the SER of the SM-FDR systems with ideal and imperfect hardware are very similar. However, when k increases, the SER of the TAS-SM-FDR system with HI increases significantly. Particularly, when k reaches 0.3, there is little difference between SERs of two cases: with and without TAS. It can also be seen in Fig. 7 that the impact of HI on the SER of the TAS-SM-FDR system is stronger than that of the non-TAS case. For the considered range of HI level (k from 0.05 to 0.3), SER of the TAS-SM-FDR changes from 8×10^{-6} to 2×10^{-2}, while SER of the non-TAS system changes from 4×10^{-3} to 2.5×10^{-2}, respectively. From Fig. 6 and Fig. 7, we can conclude that if TAS is not used, the impact of RSI (l) is stronger than that of HI (k). However, for TAS-SM-FDR system, the impact of RSI (l) is weaker than that of HI (k).

V. CONCLUSION

Transmit antenna selection is well known for improving the performance of MIMO transmission, especially for spatial modulation. However, research on the utilization of TAS is still limited because of the complexity of mathematical derivation. To tackle this problem, this paper provides the thorough analysis on using TAS to improve the performance of SM-FDR system in the presence of HI. We successfully derive the mathematical expressions for system performance evaluation in terms of OP and SER. Based on these expressions, the impact of both HI and RSI on the system performance is carefully investigated. Numerical results show that TAS greatly enhances the OP and SER performance of the considered system. Regarding the HI, its effect on TAS-SM-FDR system is more severe at higher data transmission rate. Moreover, the performance of the TAS-SM-FDR system in the presence of HI is even better than

the non-TAS-SM-FDR system with ideal hardware. Therefore, the usage of TAS is necessary to improve the performance of the SM-FDR system with HI. Additionally, without TAS, the impact of RSI is stronger than that of HI while it is weaker when TAS is applied. In conclusion, it is advisable to apply not only all SIC techniques for FD transmission but also all analog and digital signal processing methods to remove HI from physical transceivers in order to improve the system performance. In the future, this work can be developed further by applying advanced techniques to enhance the spectrum efficiency such as non-orthogonal multiple access (NOMA) or to use energy more effectively such as energy harvesting, which are currently the focusing points of 5G communication research.

APPENDIXES
APPENDIX A
This appendix provides step-by-step for the mathematical derivation of OP for the proposed TAS-SM-FDR system in Theorem 1.

For both cases with and without TAS, we need to compute the probability $\Pr\{\gamma_R < \gamma_{th1}\}$. By applying (10), we can write

$$\Pr\{\gamma_R < \gamma_{th1}\} = \Pr\left\{\|\mathbf{h}_{iR}\|^2(1 - k_S^2\gamma_{th1}) < \frac{\gamma_{th1}}{\bar{\gamma}_R}\right\}. \quad (27)$$

If $1 - k_S^2\gamma_{th1} \leq 0$, i.e. $\gamma_{th1} \geq 1/k_S^2$, the event in the left-hand side of (27) always occurs as $\|\mathbf{h}_{iR}\|^2(1 - k_S^2\gamma_{th1}) \leq 0$ while $\frac{\gamma_{th1}}{\bar{\gamma}_R} > 0$. Therefore,

$$\Pr\{\gamma_R < \gamma_{th1}\} = 1, \quad \text{when } \gamma_{th1} \geq 1/k_S^2. \quad (28)$$

Reversely, if $1 - k_S^2\gamma_{th1} > 0$, i.e. $\gamma_{th1} < 1/k_S^2$, (27) can be rewritten as

$$\Pr\{\gamma_R < \gamma_{th1}\} = \Pr\left\{\|\mathbf{h}_{iR}\|^2 < \frac{\gamma_{th1}}{\bar{\gamma}_R(1 - k_S^2\gamma_{th1})}\right\}. \quad (29)$$

To calculate the probability in (29), we start with the probability density function (PDF, denoted by $f(.)$) and the cumulative distribution function (CDF, denoted by $F(.)$) of the instantaneous channel gain amplitude, which follows Rayleigh distribution. For single channel gain, the CDF and PDF of its squared-amplitude, i.e., $|h|^2$, are given respectively as

$$F_{|h|^2}(x) = \Pr\{|h|^2 < x\} = 1 - \exp\left(-\frac{x}{\Omega}\right), \quad x \geq 0, \quad (30)$$

$$f_{|h|^2}(x) = \frac{1}{\Omega}\exp\left(-\frac{x}{\Omega}\right), \quad x \geq 0, \quad (31)$$

where $\Omega = \mathbb{E}\{|h|^2\}$ is the average of $|h|^2$; $\mathbb{E}$ is the expectation operator. In this paper, we normalize $\Omega = 1$ for all channel gains.

In the case that there are N_r receive antennas (N_{rR} at R and N_{rD} at D for the considered system) and MRC is applied at the receivers, the equivalent *SNR* at receiver is equal to the sum of *SNR*s of all receiver branches. Therefore, it's necessary to determine the sum of N_{rR} channel power gains at R and the sum of N_{rD} channel power gains at D. For example, let's

consider the sum of N_{rR} channel power gains at R, which is denoted by A_i:

$$A_i = \|\mathbf{h}_{iR}\|^2 = |h_{i1}|^2 + |h_{i2}|^2 + \ldots + |h_{iN_{rR}}|^2 = \sum_{p=1}^{N_{rR}} |h_{ip}|^2. \tag{32}$$

The CDF and PDF of A_i are respectively given by [2]:

$$F_{A_i}(x) = 1 - e^{-x} \sum_{p=0}^{N_{rR}-1} \frac{x^p}{p!}, \quad x \geq 0, \tag{33}$$

$$f_{A_i}(x) = \frac{x^{N_{rR}-1} e^{-x}}{\Gamma(N_{rR})}, \quad x \geq 0, \tag{34}$$

where $\Gamma(.)$ is the gamma function, which is defined as $\Gamma(x) \triangleq \int_0^\infty t^{x-1} e^{-t} dt$ [29].

For TAS scheme, to select the set J_S of transmitting antennas at S, all the sums of the channel power gains A_i, $i = 1, 2, \ldots, N_{tS}$ are rearranged such as in (8). From that, $|J_S|$ antennas are selected from N_{tS} transmitting antennas to get the highest value of A_i. In the case that the order statistics are $A_1 \leq A_2 \leq \ldots \leq A_{w_S} \leq \ldots \leq A_{N_{tS}}$, the PDF of A_{w_S}, where $w_S = N_{tS} - |J_S| + 1$, is given by [31, Eq. 2.1.6]:

$$f_{A_{w_S}}(x) = \frac{1}{B(w_S, N_{tS} - w_S + 1)} \times \left(F_{A_i}(x)\right)^{w_S-1} \left(1 - F_{A_i}(x)\right)^{N_{tS}-w_S} f_{A_i}(x), \tag{35}$$

where $B(.)$ is the beta function, which is defined as $B(x, y) \triangleq \int_0^1 t^{x-1}(1-t)^{y-1} dt$ [29]. Therefore, the PDF of the received $\|\mathbf{h}_{iR}\|^2$ can be derived as [19]

$$f_{\|\mathbf{h}_{iR}\|^2}(x) = \frac{1}{N_{tS} - w_S + 1} \sum_{p=w_S}^{N_{tS}} \frac{1}{B(p, N_{tS} - p + 1)} \times \left(F_{A_i}(x)\right)^{p-1} \left(1 - F_{A_i}(x)\right)^{N_{tS}-p} f_{A_i}(x). \tag{36}$$

By substituting $F_{A_i}(x)$ and $f_{A_i}(x)$ from (33) and (34) into (36), we obtain the PDF of $\|\mathbf{h}_{iR}\|^2$ as

$$f_{\|\mathbf{h}_{iR}\|^2}(x) = \frac{1}{N_{tS} - w_S + 1} \sum_{p=w_S}^{N_{tS}} \frac{1}{B(p, N_{tS} - p + 1)}$$
$$\times \left(1 - e^{-x} \sum_{p=0}^{N_{rR}-1} \frac{x^p}{p!}\right)^{p-1} \left(e^{-x} \sum_{p=0}^{N_{rR}-1} \frac{x^p}{p!}\right)^{N_{tS}-p}$$
$$\times \frac{x^{N_{rR}-1} e^{-x}}{\Gamma(N_{rR})}. \tag{37}$$

Now, by applying the finite sums [29], i.e.,

$$\sum_{p=0}^{N_{rR}-1} \frac{x^p}{p!} = e^x \frac{\Gamma(N_{rR}, x)}{\Gamma(N_{rR})}, \tag{38}$$

where $\Gamma(s, x) \triangleq \int_x^\infty t^{s-1} e^{-t} dt$ is the incomplete gamma function [29], (37) can be rewritten as

$$f_{\|\mathbf{h}_{iR}\|^2}(x)$$
$$= \frac{1}{N_{tS} - w_S + 1} \sum_{p=w_S}^{N_{tS}} \frac{1}{B(p, N_{tS} - p + 1)}$$
$$\times \left(1 - \frac{\Gamma(N_{rR}, x)}{\Gamma(N_{rR})}\right)^{p-1} \left(\frac{\Gamma(N_{rR}, x)}{\Gamma(N_{rR})}\right)^{N_{tS}-p} \cdot \frac{x^{N_{rR}-1} e^{-x}}{\Gamma(N_{rR})}. \tag{39}$$

Now, the OP of TAS-SM-FDR can be computed as

$$\mathcal{P}_{out_1} = \Pr\left\{\|\mathbf{h}_{iR}\|^2 < \frac{\gamma_{th1}}{\bar{\gamma}_R(1 - k_S^2 \gamma_{th1})}\right\}$$
$$= \int_0^{\frac{\gamma_{th1}}{\bar{\gamma}_R(1 - k_S^2 \gamma_{th1})}} f_{\|\mathbf{h}_{iR}\|^2}(x) dx$$
$$= \frac{1}{(N_{tS} - w_S + 1)\Gamma(N_{rR})} \sum_{p=w_S}^{N_{tS}} \frac{1}{B(p, N_{tS} - p + 1)}$$
$$\times \int_0^{\frac{\gamma_{th1}}{\bar{\gamma}_R(1 - k_S^2 \gamma_{th1})}} \left(1 - \frac{\Gamma(N_{rR}, x)}{\Gamma(N_{rR})}\right)^{p-1}$$
$$\times \left(\frac{\Gamma(N_{rR}, x)}{\Gamma(N_{rR})}\right)^{N_{tS}-p} x^{N_{rR}-1} e^{-x} dx. \tag{40}$$

By applying the Gaussian-Chebyshev quadrature method [32], the integral in (40) is resolved as

$$\int_0^{\frac{\gamma_{th1}}{\bar{\gamma}_R(1 - k_S^2 \gamma_{th1})}} \left(1 - \frac{\Gamma(N_{rR}, x)}{\Gamma(N_{rR})}\right)^{p-1}$$
$$\times \left(\frac{\Gamma(N_{rR}, x)}{\Gamma(N_{rR})}\right)^{N_{tS}-p} x^{N_{rR}-1} e^{-x} dx$$
$$= \frac{\pi \gamma_{th1}}{2M \bar{\gamma}_R(1 - k_S^2 \gamma_{th1})} \sum_{m=1}^M \sqrt{1 - \phi_m^2} \left(1 - \frac{\Gamma(N_{rR}, \chi_R)}{\Gamma(N_{rR})}\right)^{p-1}$$
$$\times \left(\frac{\Gamma(N_{rR}, \chi_R)}{\Gamma(N_{rR})}\right)^{N_{tS}-p} \chi_R^{N_{rR}-1} e^{-\chi_R}, \tag{41}$$

where M, ϕ_m, and χ_R are defined as in Theorem 1.

Finally, we can substitute (41) into (40) to get $\mathcal{P}_{out_1}$ for the case that $\gamma_{th1} < 1/k_S^2$ and then obtain (20) in Theorem 1.

Similarly, we can derive $\mathcal{P}_{out_2}$ as in (21) in Theorem 1. The proof is complete. ∎

APPENDIX B

In this appendix, all steps to derive SER expression of the proposed TAS-SM-FDR system are explained. To calculate SER from (23), $F(x)$ is required for this system. From the definitions of $F(x)$ and OP, i.e. $F(x) = \Pr\{\gamma_{e2e} < x\}$ and $\mathcal{P}_{out} = \Pr\{\gamma_{e2e} < \gamma_{th}\}$, we can obtain $F(x)$ from OP by replacing γ_{th} by x in the OP expression.

Specifically, by replacing γ_{th1} and γ_{th2} in (19) in Theorem 1 by x, we obtain:

$$F(x) = \begin{cases} F_{S,R}(x) + F_{R,D}(x) - F_0(x), & x < \Delta, \\ 1, & x \geq \Delta, \end{cases} \quad (42)$$

where $\Delta = \min(\frac{1}{k_S^2}, \frac{1}{k_R^2})$; $F_{A,B}(x)$ (for $(A, B) \in \{(S, R), (R, D)\}$ and $F_0(x)$ are calculated as in (43) and (44), as shown at the bottom of this page, respectively; $\psi_R = \frac{1}{2\bar{\gamma}_R}(1 + \phi_m)$ and $\psi_D = \frac{1}{2\bar{\gamma}_D}(1 + \phi_n)$. As a result, we have $\chi_R = \frac{\psi_R x}{1 - k_S^2 x}$ and $\chi_D = \frac{\psi_D x}{1 - k_R^2 x}$.

By substituting $F(x)$ in (42) into (23), we have

$$\text{SER} = \frac{a\sqrt{b}}{2\sqrt{2\pi}} \left[\int_0^\Delta \frac{e^{-bx/2}}{\sqrt{x}} F_{S,R}(x)dx + \int_0^\Delta \frac{e^{-bx/2}}{\sqrt{x}} F_{R,D}(x)dx \right.$$
$$\left. - \int_0^\Delta \frac{e^{-bx/2}}{\sqrt{x}} F_0(x)dx + \int_\Delta^\infty \frac{e^{-bx/2}}{\sqrt{x}} dx \right]. \quad (45)$$

Denote $\text{SER}_{S,R}$, $\text{SER}_{R,D}$ and SER_0 as the first, the second, and the third integrals in (45), respectively, then they can be derived as in (46), as shown at the bottom of

$$F_{A,B}(x) = \frac{\pi x^{N_{rB}}}{2C_{A,B}(N_{tA} - w_A + 1)\Gamma(N_{rB})\bar{\gamma}_B(1 - k_A^2 x)^{N_{rB}}} \sum_{p=w_A}^{N_{tA}} \sum_{m=1}^{C_{A,B}} \frac{\sqrt{1 - \phi_{A,B}^2}}{B(p, N_{tA} - p + 1)}$$
$$\times \left(1 - \frac{\Gamma(N_{rB}, \frac{\psi_B x}{1 - k_A^2 x})}{\Gamma(N_{rB})} \right)^{p-1} \left(\frac{\Gamma(N_{rB}, \frac{\psi_B x}{1 - k_A^2 x})}{\Gamma(N_{rB})} \right)^{N_{tA} - p} \psi_B^{N_{rB} - 1} e^{-\frac{\psi_B x}{1 - k_B^2 x}} \quad (43)$$

for $(A, B) \in \{(S, R), (R, D)\}$; $C_{A,B} = C_{S,R}$ or $C_{A,B} = C_{R,D}$ with $C_{S,R} = M$, $C_{R,D} = N$, $\phi_{S,R} = \phi_m$, $\phi_{R,D} = \phi_n$.

$$F_0(x) = \frac{\pi^2 x^{N_{rR} + N_{rD}}}{4MN(N_{tS} - w_S + 1)(N_{tR} - w_R + 1)\Gamma(N_{rR})\Gamma(N_{rD})\bar{\gamma}_R\bar{\gamma}_D} \sum_{p=w_S}^{N_{tS}} \sum_{m=1}^{M} \sum_{q=w_R}^{N_{tR}} \sum_{n=1}^{N} \frac{\psi_R^{N_{rR} - 1} \psi_D^{N_{rD} - 1} \sqrt{(1 - \phi_m^2)(1 - \phi_n^2)}}{B(p, N_{tS} - p + 1)B(q, N_{tR} - q + 1)}$$
$$\times \frac{e^{-\frac{\psi_R x}{1 - k_S^2 x} - \frac{\psi_D x}{1 - k_R^2 x}}}{(1 - k_S^2 x)^{N_{rR}}(1 - k_R^2 x)^{N_{rD}}} \left(1 - \frac{\Gamma(N_{rR}, \frac{\psi_R x}{1 - k_S^2 x})}{\Gamma(N_{rR})} \right)^{p-1} \left(\frac{\Gamma(N_{rR}, \frac{\psi_R x}{1 - k_S^2 x})}{\Gamma(N_{rR})} \right)^{N_{tS} - p}$$
$$\times \left(1 - \frac{\Gamma(N_{rD}, \frac{\psi_D x}{1 - k_R^2 x})}{\Gamma(N_{rD})} \right)^{q-1} \left(\frac{\Gamma(N_{rD}, \frac{\psi_D x}{1 - k_R^2 x})}{\Gamma(N_{rD})} \right)^{N_{tR} - q}. \quad (44)$$

$$\text{SER}_{A,B} = \int_0^\Delta \frac{e^{-bx/2}}{\sqrt{x}} F_{A,B}(x)dx \quad (46)$$

$$= \int_0^\Delta \frac{\pi x^{N_{rB} - \frac{1}{2}}}{2C_{A,B}(N_{tA} - w_A + 1)\Gamma(N_{rB})\bar{\gamma}_B(1 - k_A^2 x)^{N_{rB}}} \sum_{p=w_A}^{N_{tA}} \sum_{m=1}^{C_{A,B}} \frac{\sqrt{1 - \phi_{A,B}^2}}{B(p, N_{tA} - p + 1)}$$
$$\times \left(1 - \frac{\Gamma(N_{rB}, \frac{\psi_B x}{1 - k_A^2 x})}{\Gamma(N_{rB})} \right)^{p-1} \left(\frac{\Gamma(N_{rB}, \frac{\psi_B x}{1 - k_A^2 x})}{\Gamma(N_{rB})} \right)^{N_{tA} - p} \psi_B^{N_{rA} - 1} e^{-\frac{\psi_B x}{1 - k_A^2 x} - \frac{bx}{2}} dx$$

$$= \frac{\pi}{2C_{A,B}(N_{tA} - w_A + 1)\Gamma(N_{rB})\bar{\gamma}_B} \sum_{p=w_A}^{N_{tA}} \sum_{m=1}^{C_{A,B}} \frac{\psi_B^{N_{rB} - 1}\sqrt{1 - \phi_{A,B}^2}}{B(p, N_{tA} - p + 1)}$$
$$\times \int_0^\Delta \left(1 - \frac{\Gamma(N_{rB}, \frac{\psi_B x}{1 - k_A^2 x})}{\Gamma(N_{rB})} \right)^{p-1} \left(\frac{\Gamma(N_{rR}, \frac{\psi_R x}{1 - k_A^2 x})}{\Gamma(N_{rB})} \right)^{N_{tA} - p} e^{-\frac{\psi_B x}{1 - k_A^2 x} - \frac{bx}{2}} \frac{x^{N_{rB} - \frac{1}{2}}}{(1 - k_A^2 x)^{N_{rB}}} dx$$

$$= \frac{\pi^2 \Delta}{4C_{A,B}C(N_{tA} - w_A + 1)\Gamma(N_{rB})\bar{\gamma}_B} \sum_{p=w_A}^{N_{tA}} \sum_{m=1}^{C_{A,B}} \sum_{c=1}^{C} \frac{\psi_B^{N_{rB} - 1}\sqrt{(1 - \phi_{A,B}^2)(1 - \phi_c^2)}}{B(p, N_{tA} - p + 1)}$$
$$\times \left(1 - \frac{\Gamma(N_{rB}, \frac{\psi_B u}{1 - k_A^2 u})}{\Gamma(N_{rB})} \right)^{p-1} \left(\frac{\Gamma(N_{rB}, \frac{\psi_B u}{1 - k_A^2 u})}{\Gamma(N_{rB})} \right)^{N_{tA} - p} e^{-\frac{\psi_B u}{1 - k_A^2 u} - \frac{bu}{2}} \frac{u^{N_{rB} - \frac{1}{2}}}{(1 - k_A^2 u)^{N_{rB}}},$$

for $(A, B) \in \{(S, R), (R, D)\}$ and $C_{S,R} = M$, $C_{R,D} = N$, $\phi_{S,R} = \phi_m$, $\phi_{R,D} = \phi_n$.

$$
\begin{aligned}
\mathrm{SER}_0 &= \int_0^\Delta \frac{e^{-bx/2}}{\sqrt{x}} F_0(x)\, dx \\
&= \int_0^\Delta \frac{\pi^2 x^{N_{\mathrm{rR}}+N_{\mathrm{rD}}-\frac{1}{2}}}{4MN(N_{\mathrm{tS}}-w_{\mathrm{S}}+1)(N_{\mathrm{tR}}-w_{\mathrm{R}}+1)\Gamma(N_{\mathrm{rR}})\Gamma(N_{\mathrm{rD}})\bar\gamma_{\mathrm{R}}\bar\gamma_{\mathrm{D}}} \sum_{p=w_{\mathrm{S}}}^{N_{\mathrm{tS}}}\sum_{m=1}^{M}\sum_{q=w_{\mathrm{R}}}^{N_{\mathrm{tR}}}\sum_{n=1}^{N} \frac{\psi_{\mathrm{R}}^{N_{\mathrm{rR}}-1}\psi_{\mathrm{D}}^{N_{\mathrm{rD}}-1}}{B(p,N_{\mathrm{tS}}-p+1)} \\
&\quad\times \frac{\sqrt{(1-\phi_m^2)(1-\phi_n^2)}\, e^{-\frac{\psi_{\mathrm{R}}x}{1-k_{\mathrm{S}}^2 x}-\frac{\psi_{\mathrm{D}}x}{1-k_{\mathrm{R}}^2 x}-\frac{bx}{2}}}{B(q,N_{\mathrm{tR}}-q+1)(1-k_{\mathrm{S}}^2 x)^{N_{\mathrm{rR}}}(1-k_{\mathrm{R}}^2 x)^{N_{\mathrm{rD}}}} \left(1-\frac{\Gamma(N_{\mathrm{rR}},\frac{\psi_{\mathrm{R}}x}{1-k_{\mathrm{S}}^2 x})}{\Gamma(N_{\mathrm{rR}})}\right)^{p-1} \left(\frac{\Gamma(N_{\mathrm{rR}},\frac{\psi_{\mathrm{R}}x}{1-k_{\mathrm{S}}^2 x})}{\Gamma(N_{\mathrm{rR}})}\right)^{N_{\mathrm{tS}}-p} \\
&\quad\times \left(1-\frac{\Gamma(N_{\mathrm{rD}},\frac{\psi_{\mathrm{D}}x}{1-k_{\mathrm{R}}^2 x})}{\Gamma(N_{\mathrm{rD}})}\right)^{q-1} \left(\frac{\Gamma(N_{\mathrm{rD}},\frac{\psi_{\mathrm{D}}x}{1-k_{\mathrm{R}}^2 x})}{\Gamma(N_{\mathrm{rD}})}\right)^{N_{\mathrm{tR}}-q} dx \\
&= \frac{\pi^2}{4MN(N_{\mathrm{tS}}-w_{\mathrm{S}}+1)(N_{\mathrm{tR}}-w_{\mathrm{R}}+1)\Gamma(N_{\mathrm{rR}})\Gamma(N_{\mathrm{rD}})\bar\gamma_{\mathrm{R}}\bar\gamma_{\mathrm{D}}} \sum_{p=w_{\mathrm{S}}}^{N_{\mathrm{tS}}}\sum_{m=1}^{M}\sum_{q=w_{\mathrm{R}}}^{N_{\mathrm{tR}}}\sum_{n=1}^{N} \frac{\psi_{\mathrm{R}}^{N_{\mathrm{rR}}-1}\psi_{\mathrm{D}}^{N_{\mathrm{rD}}-1}}{B(p,N_{\mathrm{tS}}-p+1)} \\
&\quad\times \frac{\sqrt{(1-\phi_m^2)(1-\phi_n^2)}}{B(q,N_{\mathrm{tR}}-q+1)} \int_0^\Delta \frac{e^{-\frac{\psi_{\mathrm{R}}x}{1-k_{\mathrm{S}}^2 x}-\frac{\psi_{\mathrm{D}}x}{1-k_{\mathrm{R}}^2 x}-\frac{bx}{2}}}{(1-k_{\mathrm{S}}^2 x)^{N_{\mathrm{rR}}}(1-k_{\mathrm{R}}^2 x)^{N_{\mathrm{rD}}}} \left(1-\frac{\Gamma(N_{\mathrm{rR}},\frac{\psi_{\mathrm{R}}x}{1-k_{\mathrm{S}}^2 x})}{\Gamma(N_{\mathrm{rR}})}\right)^{p-1} \left(\frac{\Gamma(N_{\mathrm{rR}},\frac{\psi_{\mathrm{R}}x}{1-k_{\mathrm{S}}^2 x})}{\Gamma(N_{\mathrm{rR}})}\right)^{N_{\mathrm{tS}}-p} \\
&\quad\times \left(1-\frac{\Gamma(N_{\mathrm{rD}},\frac{\psi_{\mathrm{D}}x}{1-k_{\mathrm{R}}^2 x})}{\Gamma(N_{\mathrm{rD}})}\right)^{q-1} \left(\frac{\Gamma(N_{\mathrm{rD}},\frac{\psi_{\mathrm{D}}x}{1-k_{\mathrm{R}}^2 x})}{\Gamma(N_{\mathrm{rD}})}\right)^{N_{\mathrm{tR}}-q} dx \\
&\approx \frac{\pi^3 \Delta}{8MNC(N_{\mathrm{tS}}-w_{\mathrm{S}}+1)(N_{\mathrm{tR}}-w_{\mathrm{R}}+1)\Gamma(N_{\mathrm{rR}})\Gamma(N_{\mathrm{rD}})\bar\gamma_{\mathrm{R}}\bar\gamma_{\mathrm{D}}} \sum_{p=w_{\mathrm{S}}}^{N_{\mathrm{tS}}}\sum_{m=1}^{M}\sum_{q=w_{\mathrm{R}}}^{N_{\mathrm{tR}}}\sum_{n=1}^{N}\sum_{c=1}^{C} \frac{\psi_{\mathrm{R}}^{N_{\mathrm{rR}}-1}\psi_{\mathrm{D}}^{N_{\mathrm{rD}}-1}}{B(p,N_{\mathrm{tS}}-p+1)} \\
&\quad\times \frac{e^{-\frac{\psi_{\mathrm{R}}u}{1-k_{\mathrm{S}}^2 u}-\frac{\psi_{\mathrm{D}}u}{1-k_{\mathrm{R}}^2 u}-\frac{bu}{2}}\sqrt{(1-\phi_m^2)(1-\phi_n^2)(1-\phi_c^2)}}{B(q,N_{\mathrm{tR}}-q+1)(1-k_{\mathrm{S}}^2 u)^{N_{\mathrm{rR}}}(1-k_{\mathrm{R}}^2 u)^{N_{\mathrm{rD}}}} \left(1-\frac{\Gamma(N_{\mathrm{rR}},\frac{\psi_{\mathrm{R}}u}{1-k_{\mathrm{S}}^2 u})}{\Gamma(N_{\mathrm{rR}})}\right)^{p-1} \left(\frac{\Gamma(N_{\mathrm{rR}},\frac{\psi_{\mathrm{R}}u}{1-k_{\mathrm{S}}^2 u})}{\Gamma(N_{\mathrm{rR}})}\right)^{N_{\mathrm{tS}}-p} \\
&\quad\times \left(1-\frac{\Gamma(N_{\mathrm{rD}},\frac{\psi_{\mathrm{D}}u}{1-k_{\mathrm{R}}^2 u})}{\Gamma(N_{\mathrm{rD}})}\right)^{q-1} \left(\frac{\Gamma(N_{\mathrm{rD}},\frac{\psi_{\mathrm{D}}u}{1-k_{\mathrm{R}}^2 u})}{\Gamma(N_{\mathrm{rD}})}\right)^{N_{\mathrm{tR}}-q}
\end{aligned}
\tag{47}
$$

this page, and (47), as shown at the top of this page, respectively.

Then, by applying [29, Eq. 3.361], the fourth term of (45) can be rewritten as

$$
\begin{aligned}
\int_\Delta^\infty \frac{e^{-bx/2}}{\sqrt{x}}\, dx &= \int_0^\infty \frac{e^{-bx/2}}{\sqrt{x}}\, dx - \int_0^\Delta \frac{e^{-bx/2}}{\sqrt{x}}\, dx \\
&= \sqrt{\frac{2\pi}{b}}\left(1-\mathrm{erf}\left(\sqrt{\frac{b\Delta}{2}}\right)\right),
\end{aligned}
\tag{48}
$$

where $\mathrm{erf}(x) \triangleq \frac{2}{\sqrt{\pi}}\int_0^x e^{-t^2}\, dt$ is the error function [29].

Finally, by substitutinging (46), (47), and (48) into (45), we obtain (24) for the TAS-SM-FDR system with HI as in Theorem 2.

This completes the proof. ∎

REFERENCES

[1] A. H. Gazestani, S. A. Ghorashi, B. Mousavinasab, and M. Shikh-Bahaei, "A survey on implementation and applications of full duplex wireless communications," *Phys. Commun.*, vol. 34, pp. 121–134, Jun. 2019.

[2] B. C. Nguyen, T. M. Hoang, and P. T. Tran, "Performance analysis of full-duplex decode-and-forward relay system with energy harvesting over Nakagami-m fading channels," *AEU Int. J. Electron. Commun.*, vol. 98, pp. 114–122, Jan. 2019.

[3] B. C. Nguyen, T. M. Hoang, P. T. Tran, and T. N. Nguyen, "Outage probability of NOMA system with wireless power transfer at source and full-duplex relay," *AEU Int. J. Electron. Commun.*, vol. 116, Mar. 2020, Art. no. 152957.

[4] D. Bharadia, E. Mcmilin, and S. Katti, "Full duplex radios," *SIGCOMM Comput. Commun. Rev.*, vol. 43, no. 4, pp. 375–386, Aug. 2013.

[5] L. Irio and R. Oliveira, "Distribution of the residual self-interference power in in-band full-duplex wireless systems," *IEEE Access*, vol. 7, pp. 57516–57526, 2019.

[6] W. Wu, J. Zhuang, W. Wang, and B. Wang, "Geometry-based statistical channel models of reflected-path self-interference in full-duplex wireless," *IEEE Access*, vol. 7, pp. 48778–48791, 2019.

[7] A. Bhowal and R. S. Kshetrimayum, "Outage probability bound of decode and forward two-way relay employing optical spatial modulation over gamma-gamma channels," *IET Optoelectron.*, vol. 13, no. 4, pp. 183–190, Aug. 2019.

[8] B. C. Nguyen and X. N. Tran, "Performance analysis of full-duplex amplify-and-forward relay system with hardware impairments and imperfect self-interference cancellation," *Wireless Commun. Mobile Comput.*, vol. 2019, pp. 1–10, Aug. 2019.

[9] B. C. Nguyen, X. N. Tran, D. T. Tran, and L. T. Dung, "Full-duplex amplify-and-forward relay system with direct link: Performance analysis and optimization," *Physical Communication*, vol. 37, Dec. 2019, Art. no. 100888.

[10] A. Koc, I. Altunbas, and E. Basar, "Two-way full-duplex spatial modulation systems with wireless powered AF relaying," *IEEE Wireless Commun. Lett.*, vol. 7, no. 3, pp. 444–447, Jun. 2018.

[11] B. C. Nguyen, X. N. Tran, and D. T. Tran, "Performance analysis of in-band full-duplex amplify-and-forward relay system with direct link," in *Proc. 2nd Int. Conf. Recent Adv. Signal Process., Telecommun. Comput. (SigTelCom)*, Jan. 2018, pp. 192–197.

[12] C. Li, Z. Chen, Y. Wang, Y. Yao, and B. Xia, "Outage analysis of the full-duplex decode-and-forward two-way relay system," *IEEE Trans. Veh. Technol.*, vol. 66, no. 5, pp. 4073–4086, May 2017.

[13] M.-T. Le, V.-D. Ngo, H.-A. Mai, X. N. Tran, and M. Di Renzo, "Spatially modulated orthogonal space-time block codes with non-vanishing determinants," *IEEE Trans. Commun.*, vol. 62, no. 1, pp. 85–99, Jan. 2014.

[14] R. Y. Mesleh, H. Haas, S. Sinanovic, C. W. Ahn, and S. Yun, "Spatial modulation," *IEEE Trans. Veh. Technol.*, vol. 57, no. 4, pp. 2228–2241, 2008.

[15] S. Narayanan, H. Ahmadi, and M. F. Flanagan, "On the performance of spatial modulation MIMO for full-duplex relay networks," *IEEE Trans. Wireless Commun.*, vol. 16, no. 6, pp. 3727–3746, Jun. 2017.

[16] P. Raviteja, Y. Hong, and E. Viterbo, "Spatial modulation in full-duplex relaying," *IEEE Commun. Lett.*, vol. 20, no. 10, pp. 2111–2114, 2016.

[17] J. Zhang, Q. Li, K. J. Kim, Y. Wang, X. Ge, and J. Zhang, "On the performance of full-duplex two-way relay channels with spatial modulation," *IEEE Trans. Commun.*, vol. 64, no. 12, pp. 4966–4982, Dec. 2016.

[18] R. Rajashekar, K. V. S. Hari, and L. Hanzo, "Antenna selection in spatial modulation systems," *IEEE Commun. Lett.*, vol. 17, no. 3, pp. 521–524, Mar. 2013.

[19] B. Kumbhani and R. Kshetrimayum, "Outage probability analysis of spatial modulation systems with antenna selection," *Electron. Lett.*, vol. 50, no. 2, pp. 125–126, Jan. 2014.

[20] F. Yarkin and I. Altunbas, "Outage performance of spatial modulation with transmit antenna selection over Nakagami-m fading channels with arbitrary m," in *Proc. 8th Int. Congr. Ultra Mod. Telecommun. Control Syst. Workshops (ICUMT)*, Oct. 2016, pp. 438–442.

[21] E. Bjornson, J. Hoydis, M. Kountouris, and M. Debbah, "Massive MIMO systems with non-ideal hardware: Energy efficiency, estimation, and capacity limits," *IEEE Trans. Inf. Theory*, vol. 60, no. 11, pp. 7112–7139, Nov. 2014.

[22] E. Bjornson, M. Matthaiou, and M. Debbah, "A new look at dual-hop relaying: Performance limits with hardware impairments," *IEEE Trans. Commun.*, vol. 61, no. 11, pp. 4512–4525, Nov. 2013.

[23] X. N. Tran, B. C. Nguyen, and D. T. Tran, "Outage probability of two-way full-duplex relay system with hardware impairments," in *Proc. 3rd Int. Conf. Recent Adv. Signal Process., Telecommun. Comput. (SigTelCom)*, Mar. 2019, pp. 135–139.

[24] A. Papazafeiropoulos, S. K. Sharma, T. Ratnarajah, and S. Chatzinotas, "Impact of residual additive transceiver hardware impairments on Rayleigh-product MIMO channels with linear receivers: Exact and asymptotic analyses," *IEEE Trans. Commun.*, vol. 66, no. 1, pp. 105–118, 2017.

[25] A. Sabharwal, P. Schniter, D. Guo, D. W. Bliss, S. Rangarajan, and R. Wichman, "In-band full-duplex wireless: Challenges and opportunities," *IEEE J. Sel. Areas Commun.*, vol. 32, no. 9, pp. 1637–1652, Sep. 2014.

[26] B. C. Nguyen, T. M. Hoang, and L. T. Dung, "Performance analysis of vehicle-to-vehicle communication with full-duplex amplify-and-forward relay over double-Rayleigh fading channels," *Veh. Commun.*, vol. 19, Oct. 2019, Art. no. 100166.

[27] J. Jeganathan, A. Ghrayeb, L. Szczecinski, and A. Ceron, "Space shift keying modulation for MIMO channels," *IEEE Trans. Wireless Commun.*, vol. 8, no. 7, pp. 3692–3703, Jul. 2009.

[28] A. Goldsmith, *Wireless Communications*. Cambridge, U.K.: Cambridge Univ. Press, 2005.

[29] A. Jeffrey and D. Zwillinger, *Table of Integrals, Series, and Products*. New York, NY, USA: Academic, 2007.

[30] O. Abbasi and A. Ebrahimi, "Cooperative NOMA with full-duplex amplify-and-forward relaying," *Trans Emerg. Tel. Tech.*, vol. 29, no. 7, p. e3421, Jul. 2018. [Online]. Available: https://onlinelibrary.wiley.com/doi/abs/10.1002/ett.3421

[31] H. A. David and H. N. Nagaraja, "Order statistics," in *Encyclopedia of Statistical Sciences*. Hoboken, NJ, USA: Wiley, 2003.

[32] F. B. Hildebrand, *Introduction to Numerical Analysis*. North Chelmsford, MA, USA: Courier Corporation, 1987.

BA CAO NGUYEN was born in Nghean, Vietnam. He received the B.S. degree from Telecommunications University, Nha Trang, Vietnam, in 2006, and the M.S. degree from the Posts and Telecommunications Institute of Technology (VNPT), Vietnam, in 2011, and the Ph.D. degree from Le Quy Don Technical University, Hanoi, Vietnam. He is currently a Lecturer with the Basis Techniques Department, Telecommunications University. His research interests include energy harvesting, full duplex, non-orthogonal multiple access, spatial modulation, signal processing, and cooperative communication.

TRAN MANH HOANG was born in November 1977. He received the B.S. degree in communication command from Telecommunications University, Ministry of Defense, Nha Trang, Vietnam, in 2002, the B.Eng. degree in electrical engineering from Le Quy Don Technical University, Hanoi, Vietnam, in 2006, the M.Eng. degree in electronics engineering from the Posts and Telecommunications Institute of Technology (VNPT), Vietnam, in 2013, and the Ph.D. degree from Le Quy Don Technical University. He is currently a Lecturer with Telecommunications University. His research interests include energy harvesting, non-orthogonal multiple access, and signal processing for wireless cooperative communications.

PHUONG T. TRAN (Member, IEEE) was born in Ho Chi Minh City, Vietnam, in 1979. He received the B.Eng. and M.Eng. degrees in electrical engineering from the Ho Chi Minh University of Technology, Ho Chi Minh City, in 2002 and 2005, respectively, and the M.S. degree in mathematics and the Ph.D. degree in electrical and computer engineering from Purdue University, USA, in 2013. In 2007, he became a Vietnam Education Foundation Fellow with Purdue University. In 2013, he joined the Faculty of Electrical and Electronics Engineering, Ton Duc Thang University, Vietnam, where he has been the Vice Dean since October 2014. His major interests are in the areas of wireless communications and network information theory.

• • •